SNO-STR-98-010

The Angular Resolution of SNO

C.J. Jillings, Queen's University

April 30, 1998

Abstract

The angular resolution of the SNO detector is key to understanding the electron-scattering signal and making comparisons between it and the the charged-current signal. This paper presents a study of the electron-scattering signal and two methods to verify that it is being properly simulated by SNOMAN.

1 Motivation and Definitions

The angular resolution is a measure of how well the detector can reconstruct the initial direction of travel of an electron. The initial direction of the electron for an electron-scattering event is almost exactly parallel to the incident neutrino direction. This direction serves as a tag identifying the event as a candidate electron-scattering event.

In order to parameterize the angular distribution of events, the following conventions have been chosen. The variable used to study angular resolution in the Monte Carlo is $\cos\theta$, where θ is the angle between the measured electron direction and the simulated initial electron direction. By using the cosine of the angle, phase space is automatically accounted for. In the Monte Carlo study of electron-scattering events, the quantity studied is $\cos\theta_{\mathrm{sun}}$. This differs only in that the initial direction of the electron is taken to be the direction from the sun to the reconstructed position of the electron-scattering event. This analysis automatically folds in effects due to uncertainty in event reconstruction.

In order to aid a quantitative analysis, two numbers were taken from the data sets: $\cos\theta_{80}$ and $\cos\theta_{50}$. These are defined such that 80% of the events will have $\cos\theta > \cos\theta_{80}$ and 50% will have $\cos\theta > \cos\theta_{50}$.

2 What Affects the Angular Resolution

The angular resolution can in principle be affected by four things: the path of the electron through the water and the resulting distribution of Cherenkov light emitted, the optics of the detector, the average photocathode efficiency of the PMTs, PMT noise rates, and the reconstruction algorithm.

2.1 Effect of the Multiple Scattering

The electron, once set in motion, undergoes many inelastic collisions in the water which cause it to lose energy and change direction. As this occurs, the direction at which Cherenkov light is emitted changes also. Therefore, the angular reconstruction of an event will necessarily have an uncertainty even given perfect optics and position reconstruction.

The SNOMAN Monte Carlo uses the EGS4code system [?] to transport electrons. EGS4 uses Molière multiple-scattering theory with small corrections at large angles to transport electrons between discrete interactions (such as Bremstrallung or Moller scattering producing a delta ray above threshold). The Čerenkov light is generated at the Čerenkov angle along the track. A simple planar interpolation is used to determine the direction of the electron in the middle of a step in EGS4.

The electron multiple-scattering distribution is a strong function of electron energy so the angular distribution will change as a function of electron energy. This is shown in figure 1 which shows the angular distribution for electrons with kinetic energies of 6, 8, 10, and 20 MeV. The angular resolution improves with increasing energy.

2.2 Detector Optics

To study the effects of detector optical parameters, a choice of how to simulate the electrons was necessary. While simulations of monoenergetic electrons at various points in the detector may be the most fundamental choice, it is not necessarily the most applicable to extracting the electron-scattering signal. Thus the simulations performed generated electrons with a distribution taken from the electron-scattering reaction itself. That is to say the energy, initial direction, and location of the electrons were sampled to model electrons scattered from ^{8}B solar neutrinos. While the electrons were generated within 7 meters of the center of the detector, a cut was imposed keeping

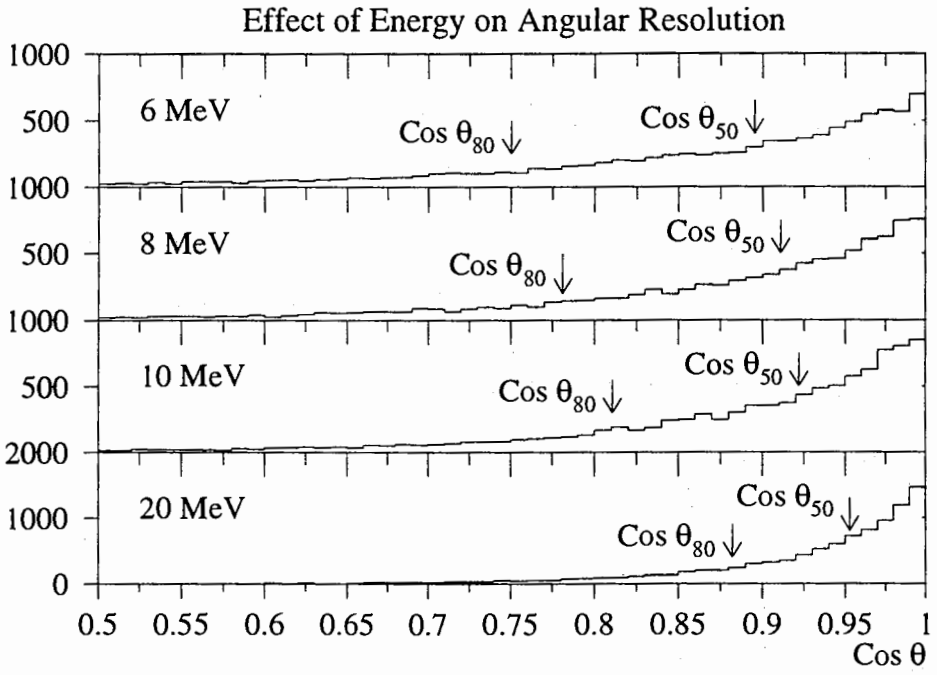

Figure 1: Angular distribution plots for monoenergetic electrons at the center of the detector. Note the increase in resolution with energy.

events that reconstructed within 6 meters of center (the heavy-water volume excluding the chimney). To average out variations caused by the location of the sun relative to the detector, the events were generated over a one year period. The simulation created events at a rate of 1100 events per day resulting in 401500 events per run.

To see the effect of detector optical properties, Monte Carlo runs were performed for various sets of optical parameters. A run was performed with "perfect" optics: the photons were allowed neither to Rayleigh scatter nor scatter diffusely from interfaces and absorption was effectively removed by setting the heavy and light water absorption lengths to 1000 meters and the acrylic absorption length to 1 meter. The histograms of angular distribution are shown in figure 2 along with the more realistic simulation with Rayleigh scattering and default absorption lengths. The value of $\cos\theta_{50}$ for the perfect

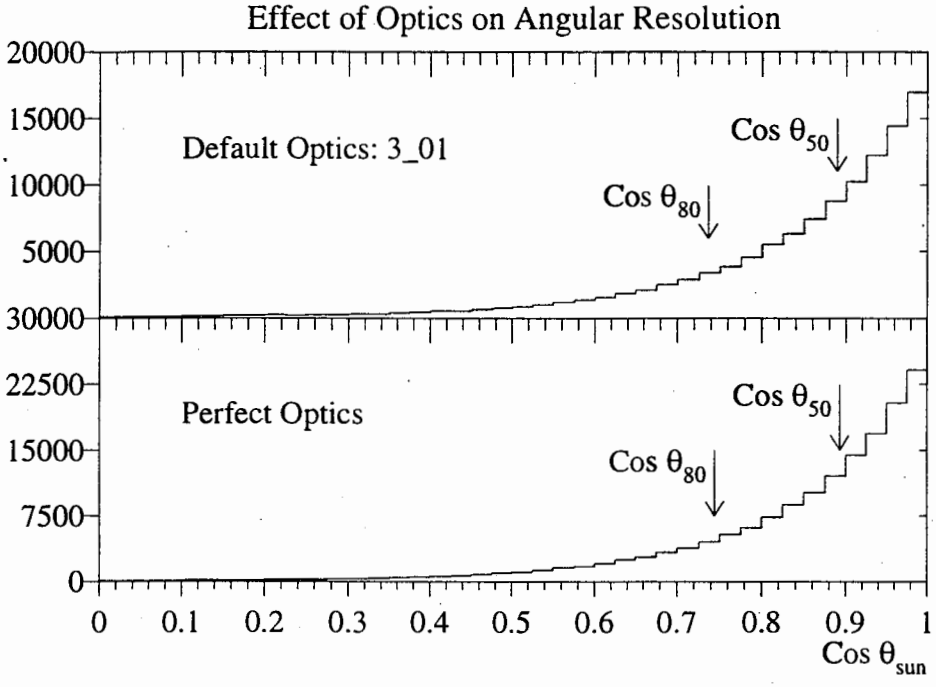

Figure 2: Angular distribution plots for electron scattering events with two different sets of optical parameters. The top plot shows the default case for SNOMAN 3.01; the bottom plot shows the case of perfect optics.

optics is 0.893; for the default case it is 0.889. The value of $\cos\theta_{80}$ for perfect optics is 0.744; for the default case it is 0.736. The effect is small.

2.3 The Average Photocathode Efficiency

The average photocathode efficiency affects the "gain" of the detector or the number of PMTs that detect light per MeV of electron energy. This effect does not discriminate between scattered or reflected and light which travels directly to a PMT (prompt light). As such, its only effect will be to increase the statistical accuracy of the reconstruction. If the electron had a large-angle scatter early in its track, the increased statistics will only serve to give a more-precise but still inaccurate initial direction. A second set of

PMT parameters was used in the simulation which increased the gain by 30%. The value of $\cos\theta_{50}$ was 0.892 and $\cos\theta_{80}$was 0.745. (The values for the default simulation were 0.889 and 0.736.) Again, the effect is small.

2.4 The Reconstruction Algorithm

2.4.1 Choice of Algorithm

The event-reconstruction algorithm, or fitter, can have profound effects on the measured angular resolution. All runs previously discussed have used a fitter which minimizes the residual in the time at which the PMTs were hit by varying the time and position of the event vertex. This "time fitter" can discard PMTs from the fit if their time residual is large enough. Only one PMT is discarded at a time and the entire minimization is re-performed before deciding whether to reject another PMT.

A second fitter was used for comparison. This "elastic fitter" is described in by S. Brice in [?]. Notice the different shape of the angular distribution. The peak is narrower but the computation time is much larger. For this reason, the histograms shown here are derived from a sample of 4000 events instead of more than 100000 like the other figures. Figure 3 shows the results.

Another relevant fitter is the "quad" fitter, developed by W. Frati [?]. It does not give directional information, but it does give better positional information than the time fitter.

The reason the elastic fitter is slow is that it requires the quad fitter to start its position-finding algorithm, and the computational expense is in the quad fitter. However, if one is willing to allow the time fitter to be less accurate in finding the reconstructed *position*, then the time fitter result can be used as an initial guess. The improved result in the *directional* reconstruction is unaffected. This is discussed in the next section.

2.4.2 The Reconstruction of Position

The reconstruction of the event position has a small impact on directional reconstruction, at least for events inside the vessel. That is to say that if one arbitrarily moved the position some tens of centimeters the reconstructed direction would be only slightly affected, at least for those events which reconstruct within the vessel.

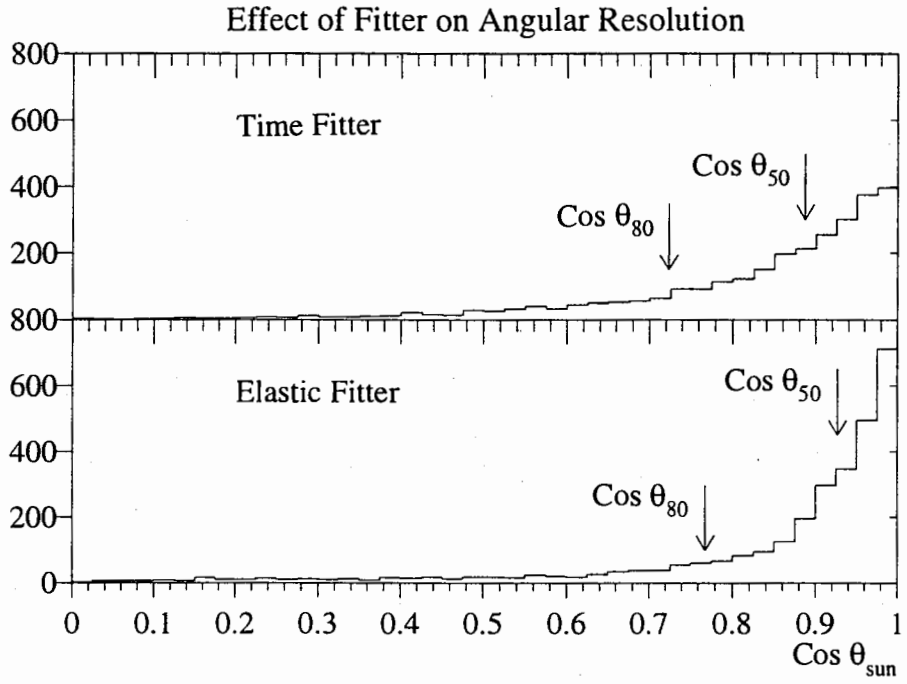

Figure 3: The angular distribution for the time fitter and elastic fitter are shown for the same event set.

2.4.3 The Pattern Of PMTs Detecting Light

However, there is an anti-correlation between accuracy in reconstructed position and direction. The root cause of the effect is the distribution of PMTs detecting light. If most of the detected light is in the Čerenkov cone, there is little information to constrain the position of the electron along its direction of travel; however, there is excellent information about the initial direction of travel. Conversely, if there are many PMTs away from the Čerenkov cone which detect light, the position of the electron is well constrained but the direction is poorly constrained.

3 Two Methods to Verify the Monte Carlo

3.1 Using a Gamma Source

To extract the electron-scattering signal, the angular resolution must be known. If SNO had a source of collimated monoenergetic electrons, we could directly measure the angular resolution. There are, however, two methods using the gamma-ray calibration sources to verify the angular resolution from the Monte Carlo.

Both methods use a gamma-ray source and study those events which reconstruct far from the source. The reason this is feasible is that for gamma rays with high energies, $E_\gamma \gg m_e$, the electron from a Compton scatter is directed preferentially parallel to the incident gamma ray. The vector from the gamma-ray source to the reconstructed vertex then defines the "true" electron direction and the fitted direction can be compared to that.

A complication is that there are multiple electrons from a single gamma ray. However, the electrons are still preferentially directed forward. A SNOMAN run was performed in which 10 MeV gamma rays were transported in the heavy water. The number of Compton scatters and pair productions were counted for each gamma, as well as the energy and momentum of each electron or positron. Several histograms were made to look at the energy flow of the charged particles. Figure 4 shows a histogram of the cosine of the angle between the initial gamma-ray direction and the electron momentum vector. But instead of adding one count to the histogram for each electron, the histogram was incremented by the electron energy less the Čerenkov threshold. This then approximates a histogram of "visible energy" against gamma direction. This is not the angular distribution.

It should also be noted that the processes by which gamma rays interact to produce energetic electrons, Compton scattering and pair production, are both well understood and intrinsically contribute no uncertainty to the technique. However, one would expect an increased width in the angular distribution for two reasons: the electrons are not perfectly parallel to the gamma rays and because the gamma-ray direction is the vector from its known point of creation to the reconstructed event vertex. This direction is uncertain because there is uncertainty in the fitted vertex and because the gamma ray can create two or more energetic electrons in two or more locations. A detailed comparison of angular distributions for electrons and gamma rays is made in a later section.

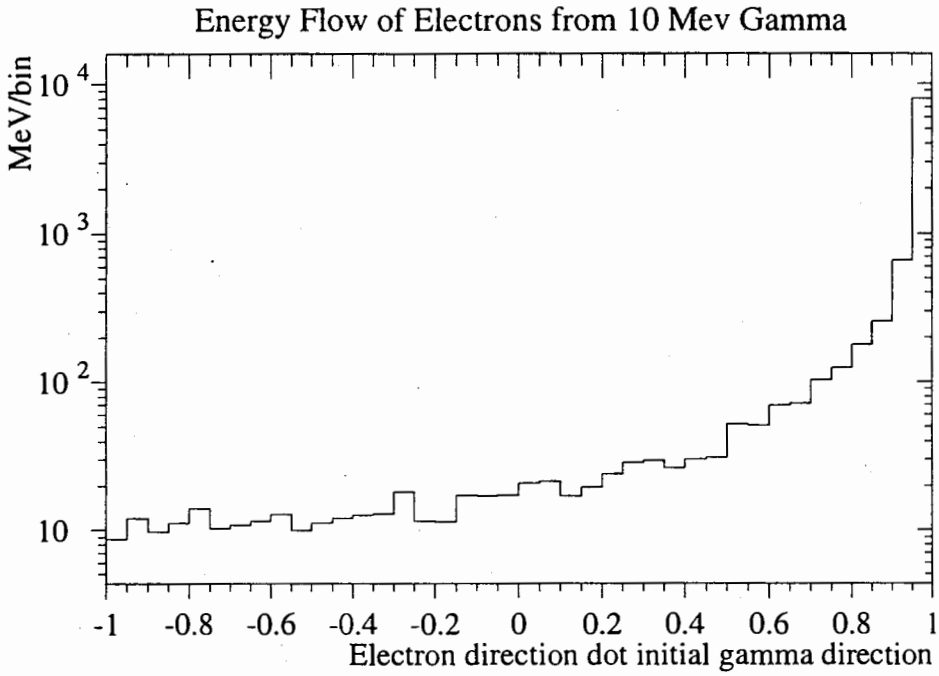

Figure 4: The direction of electrons relative to the initial gamma direction is shown. The y-axis is the amount of electron energy, above Čerenkov threshold. This is an approximation to the "visible" energy.

3.2 Method 1: The gamma source within the heavy water

The first method uses a gamma-ray source in the heavy water and relies on fitters to select those gamma rays that interact far from the source. Figure 5 shows the angular distribution for those events which reconstruct (with the time fitter) between 2 and 3 meters from the source. This peak is in fact narrower than the peak for electrons.

The cause of this narrowing is the anti-correlation discussed in section 2.4.3. Because the Compton-scattering length in water is about 40 cm for a 6.18 MeV gamma ray, the probability that a gamma travels 2 meters before interacting is e^{-5}. This number is comparable in magnitude the time-fitter

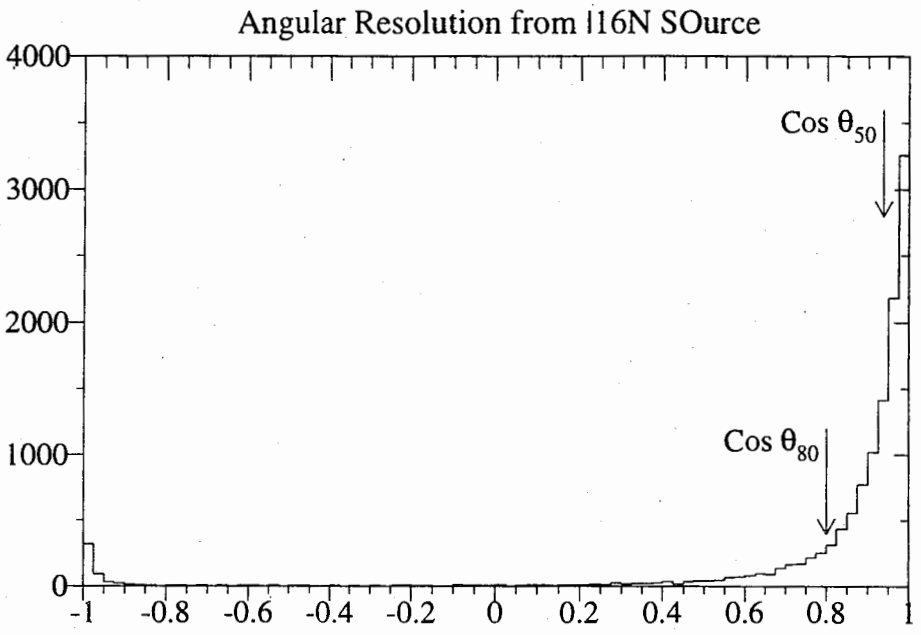

Figure 5: A histogram of angular distribution with the ^{16}N source at the origin is shown. The initial direction of the "electron" is taken to be along the vector from the gamma source to the reconstructed vertex. Only those events reconstructing between 2 and three meters from the source are included.

tail from events within 2 meters. But because these "leakage" events have a large error in reconstructed position, the direction is accurate.

To study this problem, a Monte-Carlo was performed that output the real location of the Compton scatter as well as data from the time fitter, elastic fitter and quad fitter. The "real location" of the Compton scatter requires definition because there are many electrons produced by a single gamma ray. The real position is

$$\vec{x}_{real} = \frac{E_1\vec{x_1} + E_1\vec{x_1}}{E_1 + E_2} \tag{1}$$

where E_1 and E_2 are the energies of the two most energetic electrons. Other electrons are neglected. Using this data, various cuts can be employed to

study the leakage of unwanted events into the region of interest.

The first important step is to choose a better reconstruction algorithm than the time fitter. The elastic fitter and quad fitter have reduced leakage. Also the lower bound on the radial cut was reduced to 150 cm. This increases the uncertainty in the initial direction but reduces the leakage by substantially augmenting the number of acceptable events. As well, time cut was put on events. Those events which really do reconstruct far from the source should occur later than those which occur close. This was accomplished in SNOMAN 3_0086 using the external asynchronous global trigger a known time after the event. In reality, the time will be compared to the time of the signal from the beta decay of ^{16}N. While the fitted time of an event is correlated to its fitted position, this correlation is not perfect and information is gained using the time.

Table 3.2 shows the number of good events, the number of leakage events, and the fraction of leakage events in the sample for various fitter choices.

This table makes clear that this method is very dependent on knowledge of the fitters. If they behave differently than expected, then this method may give misleading results.

4 Method 2: A Gamma Source at Partial Fill

A much cleaner signal can be obtained during partial fill. The gamma source can be hung approximately 2 meters above the water level to guarantee a long distance between the source and the interactions. There is no contamination from events close to the source. A simple cut on the fitted position being within some region of interest ensures a good data set. Also, the probability of getting an event of interest is high, approximately 20%. If there are 200 tagged gamma rays a second, then there will be 40 events a second of interest. The only drawback to this technique is it must be done during the fill and, therefore, only the ^{16}N gamma rays can be used.

A simulation of 6.18 MeV gamma rays was performed with the water level at the equator. The source was on the axis, 2 meters above the water. The number of gamma rays simulated was 100000. Figure 6 shows histograms for the time fitter and the elastic fitter.

Fitter	Time Cut	Good Events	Leakage Events	Contamination
Quad		1592	3619	0.69
Elastic	none	1582	2656	0.63
E and Q		1464	1726	0.54
Quad		1579	3356	0.68
Elastic	T_0	1562	2430	0.61
E and Q		1442	1578	0.53
Quad		1541	2816	0.65
Elastic	$T_0 + 0.5$ ns	1471	1920	0.57
E and Q		1354	1217	0.47
Quad		1420	1994	0.58
Elastic	$T_0 + 1.0$ ns	1252	1333	0.50
E and Q		1140	740	0.39
Quad		1213	1269	0.51
Elastic	$T_0 + 1.5$ ns	1003	751	0.43
E and Q		883	339	0.31
Quad		934	755	0.45
Elastic	$T_0 + 2.0$ ns	750	424	0.36
E and Q		619	183	0.22

Table 1: The ability of the fitter to separate good from leakage events. In the Monte Carlo data sample were 1879 good events and 19903 events in which the gamma rat converted outside of the region of interest. The value of T_0 is arbitrary and depends on Monte Carlo inputs. It that value of time for which the time cut starts to have an effect. If $t < T_0$, then the time cut accomplishes nothing.

5 Estimating the Statistical Accuracy needed

The ultimate point of this is to count electron-scattering events. Different MSW models suggest a change in rate of electron scattering events of about 20%. Thus, any systematic effect caused by uncertainty in the angular resolution must be small on this scale.

We need, therefore, to collect many more calibration events than real electron-scattering events, at least 10 times. We will detect approximately 300 ES events a year for a few years so we would need a few tens of thousands of calibration events. This is achievable given recent ^{16}N rates in a one to three hours.

6 A Functional Form For the Angular Resolution

6.1 Electrons with the Time Fitter

To now, the quantitative analysis of angular distributions has been the determination of the values of $\cos\theta_{80}$ and $\cos\theta_{50}$. Another approach can be taken. A functional form is derived which expresses the angular resolution as a function of energy in terms of a few parameters. This then can be used with other functions to describe the electron-scattering spectrum, for example. For a particular value of energy, E, the angular resolution is defined as

$$f(\cos\theta) = N(E) \times \left[e^{p_0(E)(\cos\theta - 1)} + p_1(E)e^{p_2(E)(\cos\theta - 1)}\right] \qquad (2)$$

where p_i are the three parameters and N is a normalization. The parameter p_0 can be understood (approximately) as the slope of a log plot of angular distribution near $\cos\theta = 1$; the parameter p_2,as the slope near $\cos\theta = 0$; and p_1 as the amplitude of the "tail". The fits to this form were performed on the range of $0 < \cos\theta < 1$. A plot (figure 7) of the angular resolution is given for a SNOMAN simulation of 8 MeV (kinetic) electrons started at the origin with an isotropic directional distribution. The time fitter was used. Note the plot has a logarithmic y-axis. There are very few counts with $\cos\theta < 1$.

A large set of parameters is still needed to determine the angular response because the p_i must be found at all energies. A series of SNOMAN runs was performed for various energies and the values of the three parameters were

extracted for each. The results are summarized in figure 8 along with fits to simple functions to describe each parameter. Thus the angular distribution for electrons has been reduced to a function of 7 parameters on the energy range from 4 to 14 MeV (kinetic).

6.2 Gamma Rays with the Time Fitter

The same exercise can be performed for gamma rays. A plot for 8 MeV gamma rays is shown in figure 9 along with the fit. A summary for gamma rays is shown in figure 10. This figure and figure 8 show that the parameters for electrons and gammas are very similar except for a shift in the energy axis.

7 Work To Be Done

There is much to be done and the schedule is tight. Analytic functions for the angular distributions derived from the elastic fitter must be found. The effect of noise rates must be understood A run plan for using the ^{16}N source must be developed before heavy water enters the vessel.

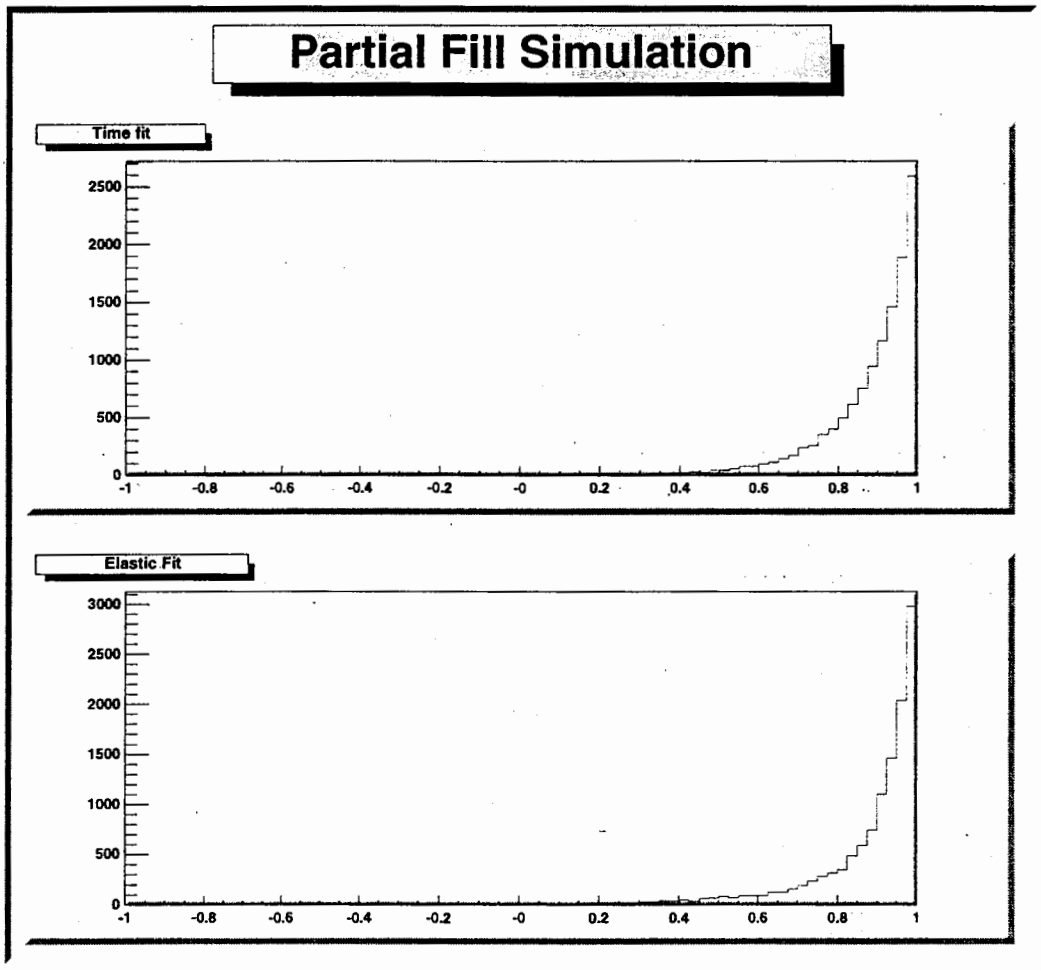

Figure 6: A histogram of angular distribution with the ^{16}N source 2 meters above the water level during partial fill. The water level is at the equator.

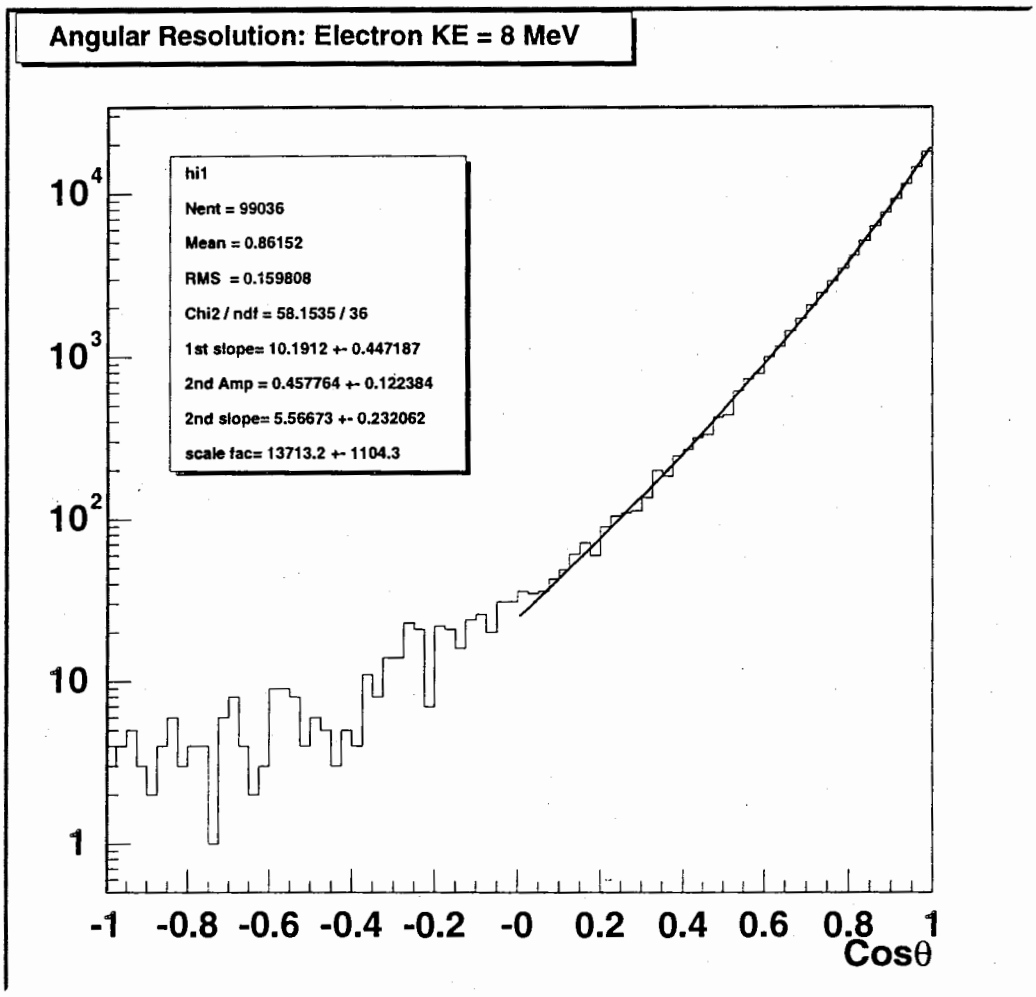

Figure 7: A histogram of the angular distribution of simulated electrons with a kinetic energy of 8 MeV is plotted with a fit to the analytic from in the text. The first slope is p_0 in the text; the second amplitude, p_1, and the second slope, p_2.

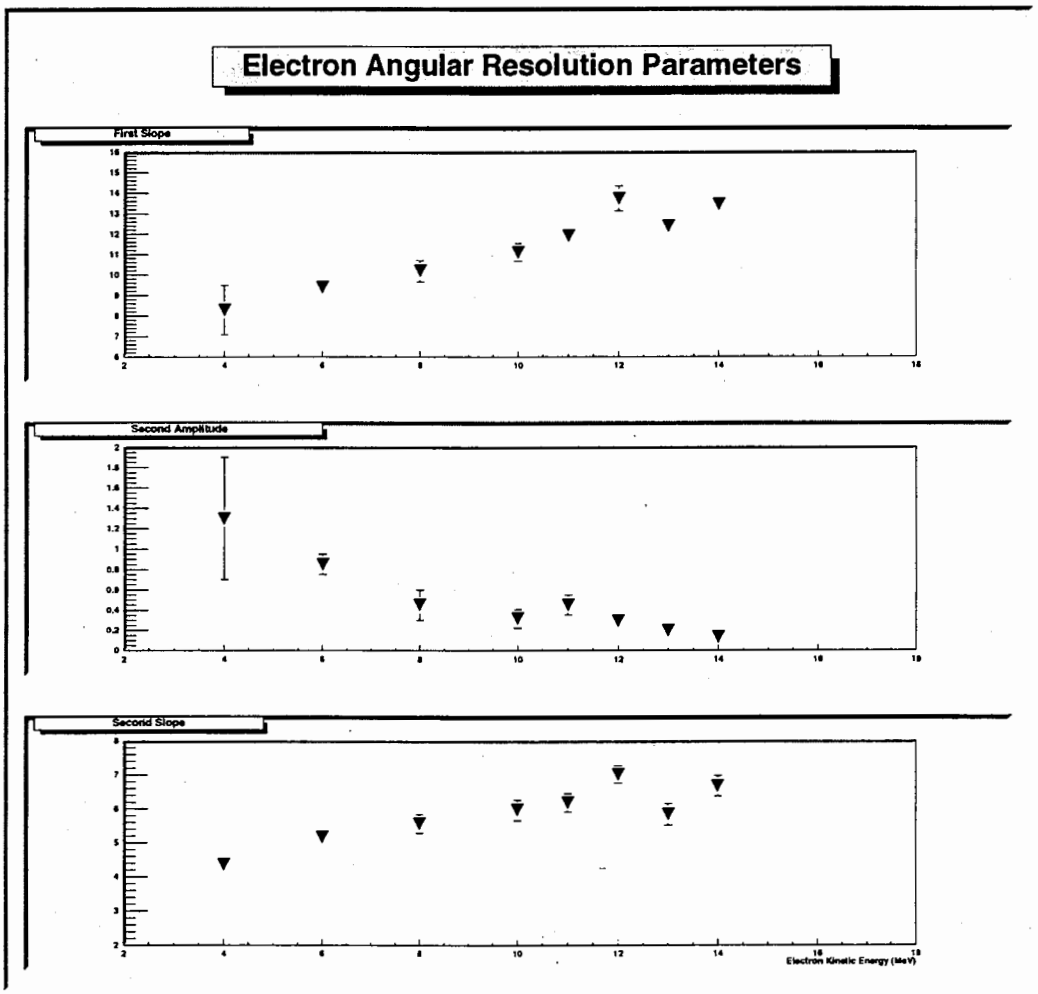

Figure 8: A summary of the electron angular distribution for time-fit 8 MeV (kinetic) electrons at the origin. The parameters plotted are those used in equation 1.

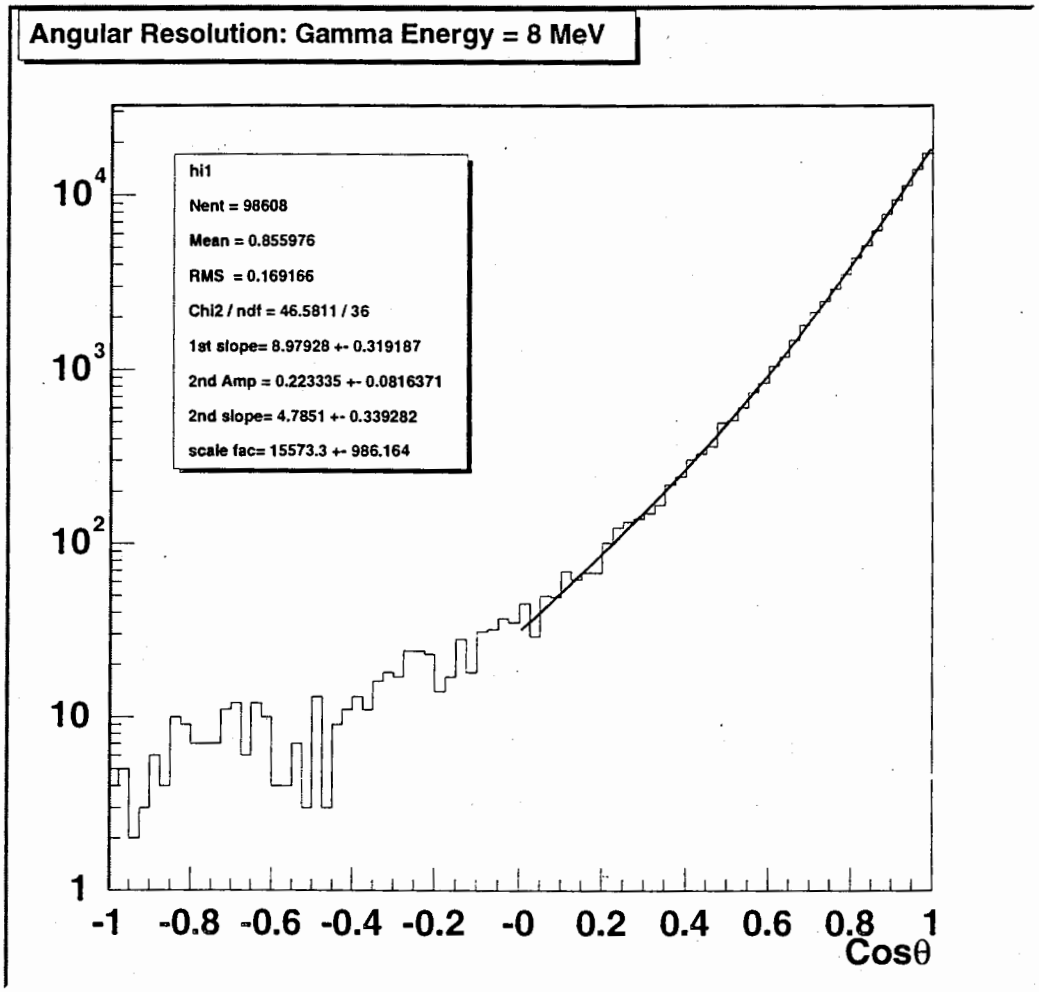

Figure 9: A histogram of the angular distribution of simulated gamma rays with an energy of 8 MeV is plotted with a fit to the analytic from in the text. The first slope is p_0 in the text; the second amplitude, p_1, and the second slope, p_2.

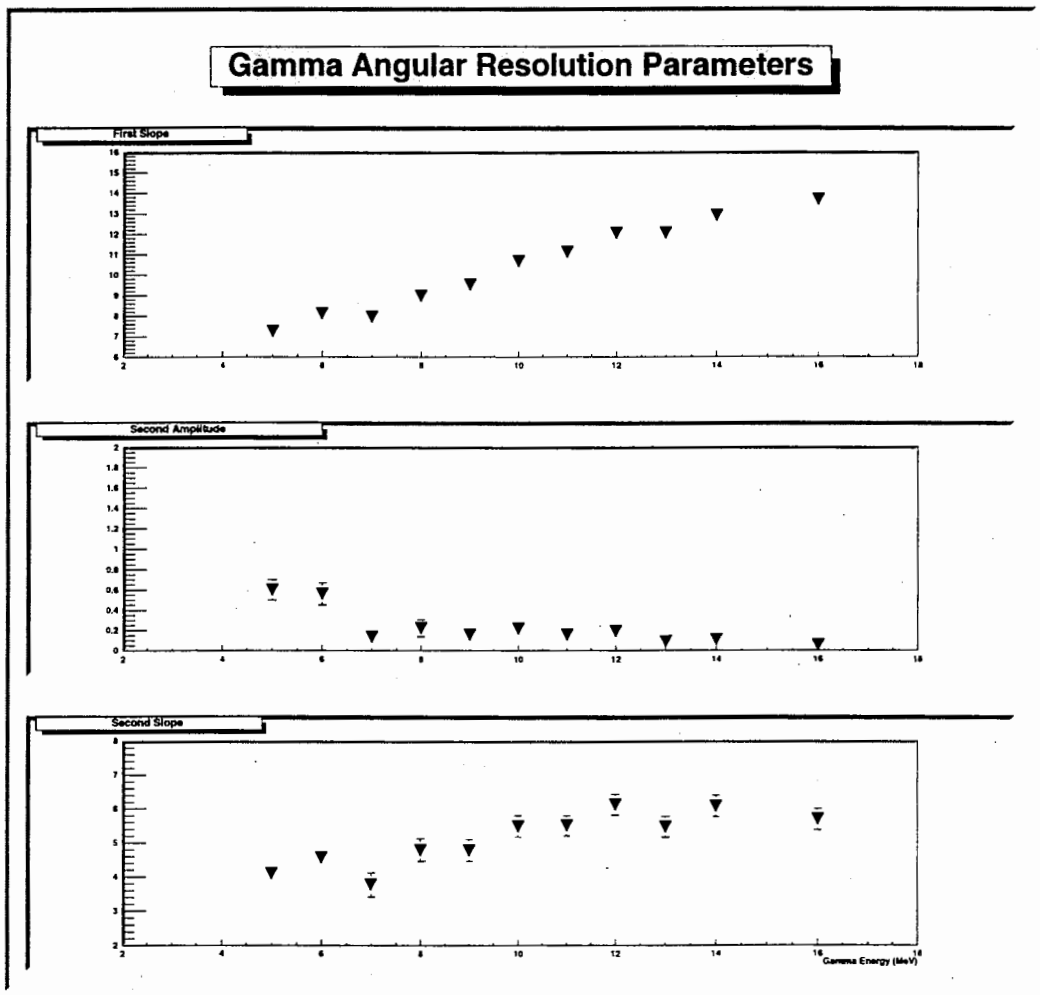

Figure 10: A summary of the gamma-ray angular distribution for time-fit 8 MeV (kinetic) electrons at the origin. The parameters plotted are those used in equation 1.